Dark matter cascade decay implications from DAMPE, HESS, Fermi-LAT and AMS02

Yu Gao[1*] and Yin-Zhe Ma[2,3†]

[1] *Key Laboratory of Particle Astrophysics,*
Institute of High Energy Physics,
Chinese Academy of Science, Beijing 100049, China
[2] *School of Chemistry and Physics,*
University of KwaZulu-Natal, Westville Campus,
Private Bag X54001, Durban, 4000, South Africa
[3] *NAOC–UKZN Computational Astrophysics Centre (NUCAC),*
University of KwaZulu-Natal, Durban, 4000, South Africa

Recent cosmic e^+e^- measurement from the *DArk Matter Particle Explorer* (*DAMPE*) satellite confirms the drop of total cosmic ray electron spectrum above 700-800 GeV. In this paper we demonstrate a $e^\pm$ signal from cascade decay of dark matter can account for *DAMPE*'s TeV e^+e^- spectrum. We select the least constraint DM decay channel into four muons as the benchmark scenario, and perform an analysis with propagation variance in both DM signal and the Milky Way's galactic electron background. A best fit is obtaint for joint *DAMPE*, Fermi-LAT, H.E.S.S. high energy electron data sets, and with a $O(10^{26})$ second decay lifetime that is consistent with existing gamma ray and cosmic microwave background limits. We comment on the spectral difference between popular cascade final states and the four muon channel's tension with sub-TeV positron data from AMS02. We also consider a more constrained four tau lepton channel as an example of further softened DM signal that is in good agreement with all four data sets.

I. INTRODUCTION

The *DArk Matter Particle Explorer* (*DAMPE*) satellite releases recent data of the combined electron and position energy spectrum [1] from $\mathcal{O}(10)$ GeV to 10 TeV in energy. The observed spectrum confirms H.E.S.S. [2] observation of a change of spectral shape at around 700-800 GeV. Below this energy the spectrum is close to a power law which is in agreement with *Fermi-LAT* [3] and H.E.S.S. [2]. But the spectrum quickly drops in the higher energy range.

The spectral change may rise from astrophysics or hypothetical new particle sources at the TeV scale. Dark matter (DM) has been a popular hypothesis [4] that can annihilate or decay into Standard Model (SM) particles. The Galactic DM halo has been widely studied to explain the observed rising of cosmic position fraction from *PAMELA* telescope [5] and later by *Fermi-LAT* [3], and *Alpha Magnetic Spectrometer* (AMS02) [6] to high precision, as well as an increase in the cosmic anti-protons [7, 8]. Alternatively, astrophysical sources such as pulsars [9–17], supernova remnants [18] are often studied as the potential sources for the positron excess. Interestingly, changes in spectral shape, indicating for a more sophisticated origin, are also observed in proton and light nuclei (see ATIC [19] and AMS02 [8]).

The dark matter hypothesis faces many constraints. While the desired electron and positron are produced from annihilation and decay processes, the associated high-energy photon radiation and inverse Compton photons can be readily searched for as diffuse or point gamma raay sources. In case of dark matter annihilation, the annihilation rate is sensitive to the DM's density distribution especially at the center of the galactic halo or sub-halos. In the directions of the Galactic Center (GC) and dwarf spheroidal galaxies (dSph), gamma ray measurement from *Fermi-LAT* [20] and H.E.S.S. [2] provided significant bounds on DM annihilation signals.

Another important bound of annihilation's impact comes from the reionization history. DM-originated e^+e^- and photons can ionize neutral hydrogen atoms after the recombination, and consequently alter the propagation of the cosmic microwave background (CMB). *Planck* 2015 data offers a severe limit on DM's zero-velocity annihilation rates [21].

In comparison, in the DM decay scenario, the strength of signal depends on the total DM abundance instead of its central density profile, thus the decay's gamma ray signal is less manifest in the direction of the galactic center, hence is less constrained. Recent studies of extragalactic diffuse photons [22] showed that DM decay channels can explain the position excess within *Fermi-LAT*'s limits. CMB constraint from *Planck* is also much weaker for DM decay due to a different redshift dependence in comparison to annihilation. Ref. [23] shows that a DM decay lifetime greater than $\mathcal{O}(10^{23-24})$s is allowed by CMB anisotropy measurements. Therefore DM decay can provide a viable candidate to explain the TeV-scale cosmic ray electron and positron dat.

In this paper, we adopt the DM cascade decay scenario, in which multiple decay steps soften the source e^+e^- spectrum and make it a suitable fit to *DAMPE*'s electron data, consistent with *Fermi-LAT*, H.E.S.S. measurements. We consider a variant power-law galactic electron background in the presence of DM decay signals. In the following, we discuss the optimal DM decay channel and galactic backgrounds in Sections II and III. Then we demonstrate the fitting result to joint

DAMPE, Fermi-LAT, HESS and AMS02 data with our cascade decay model in Section IV, and conclude in Section V.

FIG. 1: The DM decays into a pair of mediators than subsequently decay into a four-lepton final state.

II. DARK MATTER CASCADE DECAYS

Dark matter in the galactic halo decays at a constant rate that is insensitive to the dark matter particle velocity and small-scale density distribution of the density profile. With a small decay width Γ, DM decay injects SM particles at a source intensity,

$$\frac{\mathrm{d}N}{\mathrm{d}E\mathrm{d}V} = \Gamma \frac{\rho}{m_{\mathrm{DM}}} \frac{\mathrm{d}N}{\mathrm{d}E}, \qquad (1)$$

where ρ is the dark matter density, and the lifetime $\tau_{\mathrm{DM}} = \Gamma^{-1}$ needs to be much longer than the age of Universe. $\mathrm{d}N/\mathrm{d}E$ is the SM particle's energy spectrum in the decay final state, in which the maximal daughter particle energy is half the dark matter mass. To produce TeV electrons, the dark matter particle mass needs to be at least TeV scale or heavier. While photons and neutrinos can propagate to the Earth uninterruptedly, the charged particles, like $e^{\pm}, p, \bar{p}$, are affected by the galactic magnetic field and slowly diffuse away from the source in the random-walk motion.

The shape of injected e^+e^- spectrum $\mathrm{d}N/\mathrm{d}E$ is model dependent and it differs dramatically between different DM decay channels. So far the best local positron measurement is from AMS02 [6], which in the DM scenario can be dominantly from DM's contribution. Empirically the AMS02 position spectrum has a post-propagation power-law index of $\sim$-2.7 below its high-energy turn-over point[1]. This provides guidance that the DM's $e^{\pm}$ injection spectrum needs to be soft. Also, to avoid an abrupt end-point in the combined $e^{\pm}$ spectrum, which also requires the injections spectrum to be softened.

When DM directly decays into a e^+e^- pair, the injected spectrum is monochromatic and it is too hard to fit experimental data. A commonly assumed scenario, instead, is that the decay goes through of one or more intermediate decay processes, for instance, heavier lepton or hadrons that would later decay into softer electrons. Such a process is refered as a 'cascade' decay. Depending the number of immediate decays, the final electrons spectrum can vary from being hard spectrum in pair-lepton decay channel, to very soft as in hadronic showers.
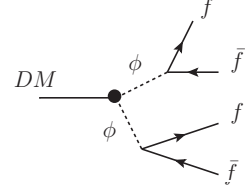
In this analysis, we adopt the cascade decay DM$\rightarrow 2\phi \rightarrow 4\mu$ as the benchmark scenario to test the *DAMPE* data. As illustrated in Fig. 1, the DM first decay into a pair of mediators that subsequently decay into four SM fermions. The fermion's injection spectrum is determined by the relative size of DM and ϕ masses, which categorizes into two typical cases: (1) a 'heavy mediator' (HM) case that $M_{\phi} \sim M_{\mathrm{DM}}$, where the ϕ pair is produced non-relativistically and each fermion carries energy equal to $M_{\phi}/2 \approx M_{\mathrm{DM}}/4$. This HM scenario can be simplistically related to a two body decay process DM$\rightarrow f\bar{f}$ with half DM mass. While the final state fermion kinematics are the same, the DM mass and injection fermion multiplicity both doubled, leading to an identical best-fit two-body decay life-time at M_{DM}. (2) a 'light-mediator' (LM) case where $M_{\phi} << M_{\mathrm{DM}}$. In this scenario, ϕ are high relativistic and its large Lorentz boost make the lab-frame spectrum of f into a plateau-shape. This softens the f spectrum, and its decay products are further softened. As the HM spectrum can be identical to a non-cascade two body spectrum, and it suffers from more severe gamma ray constraints, we only consider the LM scenario in this work.

The LM scenario has two main benefits. First, with a low ϕ mass the decay channel of ϕ can be controlled by its relative size to SM fermion masses. A scalar ϕ can preferably decay into the heaviest fermion if kinematically allowed, giving rise preference for a specific fermion. Alternatively, flavor coupling structure can also be introduced to enhance the decay branching ration into particular fermion(s), for instance by heavy non-SM gauge fields that generates a $\phi \rightarrow f\bar{f}$ at loop level [24]. As the the signal rate is insensitive to the ϕ lifetime, for galactic DM sources, a ϕ of a few GeV mass can easily evade collider and direct detection bounds if ϕ's coupling to muon and/or b-quark is small. Second and more importantly, if M_{ϕ} is near the fermion-pair mass threshold, a limited Q^2 in ϕ decay helps suppress photon radiation, and leads to diffuse reduced gamma ray constraints. By these considerations, we adopt the LM four-muon channel, where a M_{ϕ} close to $2M_{\mu}$ can provide a large 4-muon decay branching ration and reduced gamma ray radiation. In comparison, a direct $DM \rightarrow 4e$ cascade still has a hard spectral end-point, while $DM \rightarrow 4\tau$ suffers from π^0-decay photons that cannot easily evade extragalactic gamma ray bounds [22].

We illustrate the $e^{\pm}$ injection spectrum from DM$\rightarrow \phi\phi \rightarrow 4\mu$ in Fig. 2. Softer $4\tau, 4b$ cascade channels are also shown for comparison. Although the 4τ channel has severe gamma ray constraint, it produces an injection spectrum very suitable to fit the TeV-scale $e^{\pm}$ data, as will be discussed in Section IV.
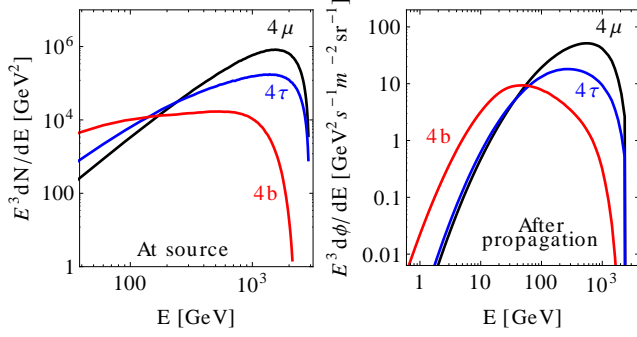
---

[1] www.ams02.org

FIG. 2: Injection $e^{\pm}$ spectra (at source, left) from four-body DM cascade decays into muons tau leptons and b-quarks. After propagation to the Earth (right), the spectra become softened due to energy loss. $M_{\mathrm{DM}} = 3\,\mathrm{TeV}$ and $M_{\phi}/M_{\mathrm{DM}} \ll 1$.

$4b$ channel represents hadronic cascade channels, which are generally two soft due to soft pion decay but also have strong associated gamma ray production.

III. $e^+ e^-$ PROPAGATION

Electrons and positions engage in diffusion motion inside the turbulent galactic magnetic field. The random-walk propagation is described by the diffusion and energy-loss equation,

$$\frac{\mathrm{d}\Phi}{\mathrm{d}t} - D(E) \cdot \nabla^2 \Phi - \partial_E(D_p(E) \cdot \Phi) = Q, \qquad (2)$$

where Φ is the cosmic ray flux and Q is the source term for astrophysical and DM injection. In the diffusion process, electrons lose energy from synchrotron radiation, inverse Compton scattering and bremsstrahlung processes, and the cosmic ray energy spectrum softens over the propagated distance. We use the GALPROP code [25, 26] in the numerical simulation of the propagation process, in which the spatial diffusion coefficient $D(E)$ is parametrized [27] as

$$D = \beta D_0 \left(\frac{R}{R_0} \right)^{\delta} \mathrm{cm}^2\,\mathrm{s}^{-1}, \qquad (3)$$

where $\beta \sim 1$ is the cosmic ray velocity. The R denotes the particle rigidity and for highly relativistic electrons it differs from energy by the electric charge. For δ we use a value above $1/3$ as is for a turbulent galactic magnetic field with a Kolmogrov spectrum. The energy-loss coefficient D_p is dynamically evaluated in the propagation process. For a reference rigidity $D_0 \sim$ GV would take values $3 \sim 5 \times 10^{28}\,\mathrm{cm}^2/\mathrm{s}$ to fit cosmic nuclei data [27].

For the DM halo distribution, we adopt the Einasto profile [28] to compute the dark matter source intensity,

$$\rho(r) = \rho_{\odot} \exp\left[-\frac{2}{\alpha} \left(\frac{r^{\alpha} - r_{\odot}^{\alpha}}{r_{\mathrm{s}}^{\alpha}} \right) \right] \qquad (4)$$

where $\rho_{\odot} = 0.3\,\mathrm{GeV/cm}^3$, $\alpha = 1.7$, $r_{\mathrm{s}} = 25$ kpc. For decaying dark matter, the choice of a cuspy or non-cuspy distribution does not qualitively affect the indirect signals, and

the Einasto profile presents an adequate example for typical cold dark matter. It is noted that the non-cuspy isothermal profile [29] is more favoured by recent N-body simulation results [30] as it would offer better agreement with the missing satellite problem [30].

Right panel in Figure 2 shows the DM's $e^{\pm}$ spectrum after propagating to the Earth. Comparing to the injection spectrum, the spectral shape becomes sufficiently softened and suitable to fit experimental data. The after-propagation curves assume a best-fit from the parameter-scan on a grid diffusion parameters,$\{D_0, \rho_0, \delta\}$. Noted that after propagation the peak of each channel's spectrum locates at different energies, and the DM mass that optimizes for a TeV cosmic ray source can be inferred by aligning the peak to *DAMPE*'s turning point, i.e. $M_{\mathrm{DM}} \sim 6\,\mathrm{TeV}$ for 4μ, 10 TeV for 4τ. The $4b$ cascade channel would require a 100TeV-scale DM mass as its propagated peak energy locates at $O(10^{-2})$ of M_{DM}.

A few comments are due for DM$\to 4b$ channel and other hadronic channnels. Hadronization in these channels contribute to a potential signal in cosmic ray anti-protons. A recent study [31] showed that in case of DM annihilation, the $b\bar{b}$ channel with a thermal cross-section would improve the fit to AMS02's antriproton data. The fit to anti-proton data can be consistent with that for the galactic center excess and CMB constraint [32]. The DM decay case has a less stringent diffuse gamma ray bound,thus its impact on the anti-protons is also important to study. Here we do not pursue it further as the 10^2 GeV mass is insufficient to fit *DAMPE* results.

IV. FIT TO *DAMPE*, FERMI-LAT, H.E.S.S. & AMS02

We perform fits to joint *DAMPE* [1], H.E.S.S. [2], Fermi-LAT 'high energy' (FermiHE) [33] and AMS02 [6] data. For data selection, we focus on the high energy part of the spectra and only include data above 80 GeV from each data set. The high-statistics data in the lower energy range can be sensitive to galactic source and propagation modeling, and may overpower the presence of a DM signal if included.

We use *DAMPE*, Fermi-LAT and and H.E.S.S. 'total electron' data (both electron and positrons) in the fit. For AMS02, as its electron flux normalizations differ from that of Fermi-LAT *DAMPE*, we give the fitting results for both including and excluding AMS02 data. When included, we fit AMS02's positron fraction data instead of the absolute flux data to avoid swelling the likelihood from normalization discrepancies between high statistics data sets.

H.E.S.S. data have large systematic uncertainty due to atmospheric hadronic modeling [2]. If naively added in quadrature, this systematic uncertainty may overwhelm the statistic uncertainty and render the H.E.S.S. spectral shape uneffective in the combined likehood analysis. Here we consider the systematic uncertainties to be correlated and adopt a scaling factor f that let the H.E.S.S. electron spectrum to float, while keeping the shape unchanged. The H.E.S.S. contribution to the total χ^2 would then only use the scaled statistic uncertainty, plus an additional term that take accounts for the scal-
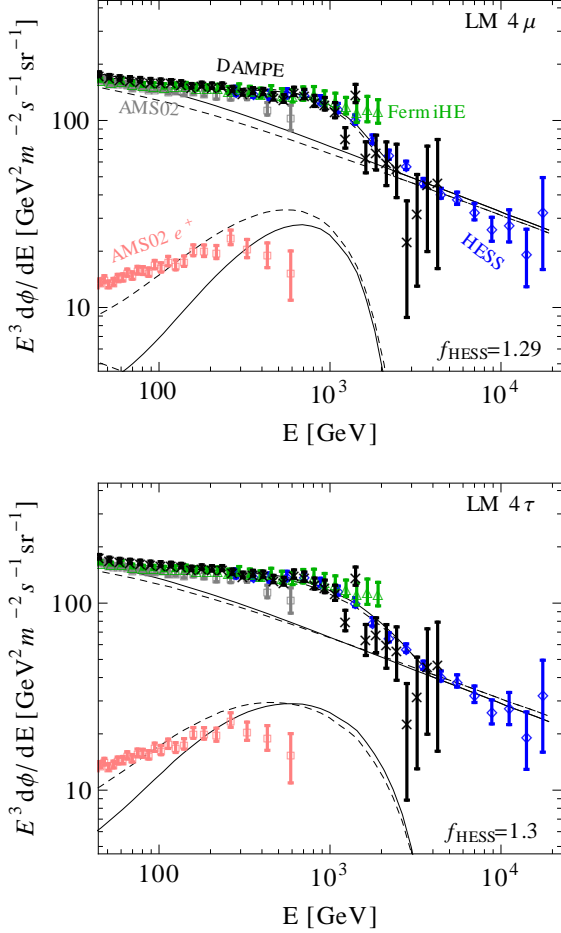
background and the DM signal contributions,

$$\phi = \phi_{bkg}(D_0, \rho_0, \delta, \phi_0, \delta_e) + \phi_{DM}(D_0, \rho_0, \delta) \qquad (6)$$

where the background cosmic electron mostly arise from supernova injection, and also includes sub-leading contributions from isotope decays. ϕ_0 is the normalization of astrophysical electron at the reference rigidity 3.45GV, and δ_e is the supernova injection power-law index above 4 GV. $\{D_0, \rho_0, \delta\}$ are the diffusion paramters in Eq. 3. For solar modulation, we adopt a fixed modulation potential at 700 MV. Noted that more complicated galactic spectral shape are possible, yet it would introduce additional degrees of freedom and makes termination of DM properties less transparent.

We adopt the scan approach and parameter range in Ref. [35] that we first obtain the propagated $e^{\pm}$ spectra on a grid on the five propagation and injection parameters. Then an interpolated total $e^{\pm}$ and position fraction spectra are fit to the combined data sets. The best-fit spectra are shown in Fig. 3 and the goodness of fit are listed in Table I.

As illustrated in Fig. 3 and Table I, the benchmark DM$\rightarrow$ $2\phi \rightarrow 4\mu$ cascade give a good fit to the shape of *DMPE*, Fermi-LAT and H.E.S.S. data, the best-fit decay lifetime is 2×10^{26}s for a 6 TeV dark matter that is allowed by extragalactic diffuse gamma ray search and CMB anisotropy constraints. The H.E.S.S. data would upscale by 30% and align with *DAMPE*, Fermi-LAT data points at the best fit. Note there is also minor difference between *DAMPE* and Fermi-LAT at above 1 TeV; if we fit only *DAMPE* and H.E.S.S datasets, a perfect 1.2σ fit of reduced χ^2 at 1.17 can be achieved.

However, the joint fit to all four data set does not produce a good best-fit. Due to a lower normalization in the AMS02 electron data, the best-fit to AMS02 would require a lower DM mass than that by *DAMPE* and H.E.S.S. spectral fall at around TeV. At 6 TeV the DM positron spectrum does not agree with the AMS02's positron measurement, making significant constribution to the total χ^2.

For comparison, the 4τ channel has a softer $e^{\pm}$ spectrum that helps fitting both AMS02 positron data and othe r data sets. A 2.1σ fit to all four data set is achieved at 10 TeV DM mass with a 6.5×10^{25}s lifetime . Although the 4τ channel can be difficult to evade gamma ray bounds, it demonstrates that a spectrum softer than $4mu$ can consistently fit AMS02 and the TeV data from *DAMPE*, H.E.S.S. and Fermi-LAT.

V. CONCLUSION

With the assumption of a power-law like galactic electron background, the cascade decay of multi-TeV DM into four leptons can accomodate for the TeV-scale shape of cosmic ray electrons as measured by *DAMPE*, H.E.S.S. and Fermi-LAT. The low-mass mediator scenarion is cascade decay reduces associated gamma ray radiation and provides softening in the injection electron/positron spectrum. We considerd a 6 TeV DM$\rightarrow 4\mu$ channel as a benchmark scenario as this channel is the least constrained by diffuse gamma ray and CMB measurements. A best fit at 2.1σ confidence level is achieved

FIG. 3: Best-fit DM$\rightarrow 2\phi \rightarrow 4\mu$ (upper), 4τ (lower) cases to total $e^{\pm}$ data from *DAMPE* and H.E.S.S., and the positron fraction data from AMS02. In each panel, the solid curves show the fit without including AMS02 data, while the dashed curves are the best-fit with AMS02 positron fraction data included. Each set of three curves are the total (DM+galactic) $e^{\pm}$, galactic $e^{\pm}$ and total e^+ spectra.

ing,

$$\chi^2_{\text{H.E.S.S.}} = \sum \frac{(\phi_i^{th} - f \cdot \phi_i^{ex})^2}{f^2 \delta\phi_i^2} + \frac{(f-1)^2}{(\delta f)^2} \qquad (5)$$

where ϕ^{th}, ϕ^{ex} denote for theoretical and measured electron flux. δf denotes the range of systematic uncertainty. Best-fits occur at $f = 1.3$ while H.E.S.S systematics error band can be 40% above measured data [34], we take $\delta f = 0.4$ in the positive direction and the additional term would only contribute a small correction ~ 0.5 to the total χ^2.

The χ^2 from each data set are simply added without additonal weighing. *DAMPE*, Fermi-LAT high energy set, H.E.S.S and AMS02 have 29, 23,19 and 14 data points above 80 GeV. Note H.E.S.S. will have one additional data point due to scaling.

We assume a single power-law spectrum for galactic electron background. The total cosmic ray spectrum consist of a

Data	DAMPE	FermiHE	H.E.S.S	DAMPE	FermiHE	H.E.S.S	AMS02
DM$\to 4\mu$	40	26	21	56	24	33	53
χ^2/#d.o.f	1.35 (2.1σ)			2.11 (5.5σ)			
DM$\to 4\tau$	42	17	14	40	23	18	21
χ^2/#d.o.f	1.12 (1.2σ)			1.30 (2.1σ)			

TABLE I: χ^2 for each data set at joint best fit. Both 4μ and 4μ channels are listed. The DM mass is 6 TeV and 10 TeV, respectively. The total number of degrees of freedom is 79(65) with(without) AMS02 data.

for joint *DAMPE*, H.E.S.S. and Fermi-LAT analysis, but does not provide a good fit to the sub-TeV AMS02 positron data at the same time. Softer cascade decay signal from the DM$\to 4\tau$ is also considered and it can explain the $e^\pm$ spectra for all four data sets. Cascade DM decay is an interesting scenario that accomendate for injection spectrum softening and avoidance of strong gamma ray emission, esp. with low mass intermediate states and decay channels with lower pion multiplicity. Further study for viable cascade decay processes will help us understand the DM explanation for the turning of cosmic ray electron spectrum in *DAMPE* and H.E.S.S. observations.

[1] G. Ambrosi, Q. An, R. Asfandiyarov, P. Azzarello, P. Bernardini, B. Bertucci, M. S. Cai, J. Chang, D. Y. Chen, H. F. Chen, et al., ArXiv e-prints (2017), 1711.10981.

[2] H. Abdalla et al. (H.E.S.S.) (2017), 1709.06442.

[3] A. A. Abdo, M. Ackermann, M. Ajello, W. B. Atwood, M. Axelsson, L. Baldini, J. Ballet, G. Barbiellini, D. Bastieri, M. Battelino, et al., Physical Review Letters **102**, 181101 (2009), 0905.0025.

[4] J. L. Feng, Annual Review of Astron and Astrophys **48**, 495 (2010), 1003.0904.

[5] O. Adriani, G. C. Barbarino, G. A. Bazilevskaya, R. Bellotti, M. Boezio, E. A. Bogomolov, M. Bongi, V. Bonvicini, S. Borisov, S. Bottai, et al., Physical Review Letters **106**, 201101 (2011), 1103.2880.

[6] M. Aguilar, G. Alberti, B. Alpat, A. Alvino, G. Ambrosi, K. Andeen, H. Anderhub, L. Arruda, P. Azzarello, A. Bachlechner, et al., Physical Review Letters **110**, 141102 (2013).

[7] O. Adriani, G. C. Barbarino, G. A. Bazilevskaya, R. Bellotti, M. Boezio, E. A. Bogomolov, L. Bonechi, M. Bongi, V. Bonvicini, S. Borisov, et al., Physical Review Letters **105**, 121101 (2010), 1007.0821.

[8] M. Aguilar, L. Ali Cavasonza, G. Ambrosi, L. Arruda, N. Attig, S. Aupetit, P. Azzarello, A. Bachlechner, F. Barao, A. Barrau, et al. (AMS Collaboration), Phys. Rev. Lett. **117**, 231102 (2016), URL https://link.aps.org/doi/10.1103/PhysRevLett.117.231102.

[9] D. Hooper, P. Blasi, and P. Dario Serpico, Journal of Cosmology and Astroparticle Physics **1**, 025 (2009), 0810.1527.

[10] H. Yüksel, M. D. Kistler, and T. Stanev, Physical Review Letters **103**, 051101 (2009), 0810.2784.

[11] K. Ioka, Progress of Theoretical Physics **123**, 743 (2010), 0812.4851.

[12] N. J. Shaviv, E. Nakar, and T. Piran, Physical Review Letters **103**, 111302 (2009), 0902.0376.

[13] N. Kawanaka, K. Ioka, and M. M. Nojiri, The Astrophysical Journal **710**, 958 (2010), 0903.3782.

[14] P. L. Biermann, J. K. Becker, A. Meli, W. Rhode, E. S. Seo, and T. Stanev, Physical Review Letters **103**, 061101 (2009), 0903.4048.

[15] P. Blasi, Physical Review Letters **103**, 051104 (2009), 0903.2794.

[16] S. Profumo, Central European Journal of Physics **10**, 1 (2012), 0812.4457.

[17] D. Malyshev, I. Cholis, and J. Gelfand, Physical Review D **80**, 063005 (2009), 0903.1310.

[18] W. Liu, X.-J. Bi, S.-J. Lin, B.-B. Wang, and P.-F. Yin, Physical Review D **96**, 023006 (2017), 1611.09118.

[19] J. Chang, J. H. Adams, H. S. Ahn, G. L. Bashindzhagyan, M. Christl, O. Ganel, T. G. Guzik, J. Isbert, K. C. Kim, E. N. Kuznetsov, et al., Nature **456**, 362 (2008).

[20] M. Ackermann, A. Albert, B. Anderson, W. B. Atwood, L. Baldini, G. Barbiellini, D. Bastieri, K. Bechtol, R. Bellazzini, E. Bissaldi, et al., Physical Review Letters **115**, 231301 (2015), 1503.02641.

[21] Planck Collaboration, P. A. R. Ade, N. Aghanim, M. Arnaud, M. Ashdown, J. Aumont, C. Baccigalupi, A. J. Banday, R. B. Barreiro, J. G. Bartlett, et al., Astronomy and Astrophysics **594**, A13 (2016), 1502.01589.

[22] W. Liu, X.-J. Bi, S.-J. Lin, and P.-F. Yin, Chinese Physics C **41**, 045104 (2017), 1602.01012.

[23] T. R. Slatyer and C.-L. Wu, Physical Review D **95**, 023010 (2017), 1610.06933.

[24] R. Allahverdi, B. Dutta, K. Richardson-McDaniel, and Y. Santoso, Physics Letters B **677**, 172 (2009), 0902.3463.

[25] A. W. Strong and I. V. Moskalenko, International Cosmic Ray Conference **4**, 255 (1999), astro-ph/9906228.

[26] A. W. Strong and I. V. Moskalenko, International Cosmic Ray Conference **5**, 1942 (2001), astro-ph/0106504.

[27] A. W. Strong, I. V. Moskalenko, and V. S. Ptuskin, Annual Review of Nuclear and Particle Science **57**, 285 (2007), astro-ph/0701517.

[28] J. Einasto, Trudy Astrofizicheskogo Instituta Alma-Ata **5**, 87 (1965).

[29] J. N. Bahcall and R. M. Soneira, The Astrophysical Journal

Supplement Series **44**, 73 (1980).

[30] J. S. Bullock and M. Boylan-Kolchin, Annual Review of Astron and Astrophys **55**, 343 (2017), 1707.04256.

[31] M.-Y. Cui, Q. Yuan, Y.-L. S. Tsai, and Y.-Z. Fan, Physical Review Letters **118**, 191101 (2017), 1610.03840.

[32] S. J. Clark, B. Dutta, and L. E. Strigari, ArXiv e-prints (2017), 1709.07410.

[33] S. Abdollahi et al. (Fermi-LAT), Phys. Rev. **D95**, 082007 (2017), 1704.07195.

[34] F. Aharonian, A. G. Akhperjanian, G. Anton, U. Barres de Almeida, A. R. Bazer-Bachi, Y. Becherini, B. Behera, K. Bernlöhr, A. Bochow, C. Boisson, et al., Astronomy and Astrophysics **508**, 561 (2009), 0905.0105.

[35] V. Barger, Y. Gao, W.-Y. Keung, D. Marfatia, and G. Shaughnessy, Physics Letters B **678**, 283 (2009), 0904.2001.

[36] K. Fang, X.-J. Bi, and P.-F. Yin, ArXiv e-prints (2017), 1711.10996.

[37] Q. Yuan, L. Feng, P.-F. Yin, Y.-Z. Fan, X.-J. Bi, M.-Y. Cui, T.-K. Dong, Y.-Q. Guo, K. Fang, H.-B. Hu, et al., ArXiv e-prints (2017), 1711.10989.

[38] Y.-Z. Fan, W.-C. Huang, M. Spinrath, Y.-L. Sming Tsai, and Q. Yuan, ArXiv e-prints (2017), 1711.10995.

[39] G. H. Duan, L. Feng, F. Wang, L. Wu, J. M. Yang, and R. Zheng, ArXiv e-prints (2017), 1711.11012.